Plant Biotechnology Journal
Open Access

Plant Biotechnology Journal (2020) **18**, pp. 1241–1254 doi: 10.1111/pbi.13288

Transcription factor BnaA9.WRKY47 contributes to the adaptation of *Brassica napus* to low boron stress by up-regulating the boric acid channel gene *BnaA3.NIP5;1*

Yingna Feng, Rui Cui, Sheliang Wang, Mingliang He, Yingpeng Hua, Lei Shi, Xiangsheng Ye and Fangsen Xu

National Key Laboratory of Crop Genetic Improvement, Microelement Research Centre, Huazhong Agricultural University, Wuhan, China

Received 2 August 2019;
revised 17 October 2019;
accepted 1 November 2019.
**Correspondence* (Tel +86-27-87282225; fax +86-27-87280016; email fangsenxu@mail.hzau.edu.cn)

Keywords: *Brassica napus*, WRKY, transcription factor, W box, boric acid channel, low B adaptation.

Summary

Boron (B) deficiency is one of the major causes of growth inhibition and yield reduction in *Brassica napus* (*B. napus*). However, the molecular mechanisms of low B adaptation in *B. napus* are largely unknown. Here, fifty-one BnaWRKY transcription factors were identified as responsive to B deficiency in *B. napus*, in which BnaAn.WRKY26, BnaA9.WRKY47, BnaA1.WKRY53 and BnaCn.WRKY57 were tested in yeast one-hybrid assays and showed strong binding activity with conserved sequences containing a W box in the promoters of the B transport-related genes *BnaNIP5;1s* and *BnaBOR1s*. Green fluorescent protein fused to the target protein demonstrated the nuclear localization of BnaA9.WRKY47. CRISPR/Cas9-mediated knockout lines of *BnaA9.WRKY47* in *B. napus* had increased sensitivity to low B and lower contents of B than wild-type plants. In contrast, overexpression of *BnaA9.WRKY47* enhanced the adaptation to low B with higher B contents in tissues than in wild-type plants. Consistent with the phenotypic response and B accumulation in these transgenic lines, the transcription activity of *BnaA3.NIP5;1,* a B efficiency candidate gene, was decreased in the knockout lines but was significantly increased in the overexpressing lines under low B conditions. Electrophoretic mobility shift assays, transient expression experiments in tobacco and in situ hybridizations showed that BnaA9.WRKY47 directly activated *BnaA3.NIP5;1* expression through binding to the specific *cis*-element. Taken together, our findings support BnaWRKYs as new participants in response to low B, and BnaA9.WRKY47 contributes to the adaptation of *B. napus* to B deficiency through up-regulating *BnaA3.NIP5;1* expression to facilitate efficient B uptake.

Introduction

As sessile organisms, plants have to quickly transduce extracellular stimuli/stresses to endogenous signals through signal transduction cascades, finally leading to physiological adaptation. During this process, numerous transcription factors serve as the switches of regulatory cascades, such as well-characterized members of MYB (myeloblastosis-related), bZIP (basic leucine zipper) and WRKY families (Spitz and Furlong, 2012). WRKY, one of the largest and most important transcription factor families, has been widely identified in various plant species and modulates many plant processes (Rushton *et al.*, 2010). The WRKY proteins contain one or two domains composed of the relatively conserved amino acid sequence WRKYGQK together with a novel zinc-finger-like motif (Ulker and Somssich, 2004). With the ability to bind specifically to T/CTGACC/T (W box) *cis*-regulatory elements present in promoters of target genes, the WRKY domains activate or repress the transcription of the target genes (Eulgem *et al.*, 2000). WRKY-mediated gene expression is involved in various stress responses, such as pathogen defence, cold resistance, salt tolerance and nutritional stresses, and in developmental and metabolic processes (Phukan *et al.*, 2016). Accumulating evidence has highlighted the importance of *WRKY* genes in responding to nutrient conditions. During phosphate (Pi) starvation, AtWRKY45 activated *PHT1* (Phosphate transporter) expression to take up Pi (Wang *et al.*, 2014). In addition, AtWRKY6 and AtWRKY42 (two suppressors of *PHO1*) were degraded to release PHO1 (Phosphate1, Pi transporter) which enhances plant Pi transfer from root to shoot (Chen *et al.*, 2009; Su *et al.*, 2015). Down-regulation of AtWRKY75 and OsWRKY74 increased the sensitivity of plants to Pi starvation (Dai *et al.*, 2016; Devaiah *et al.*, 2007). During Fe deficiency, AtWRKY46 promoted Fe translocation from root to shoot by directly up-regulating the expression of Fe transporter gene *VITL1* (Yan *et al.*, 2016).

Boron (B) is essential for plant growth, but it often limits crop production worldwide owing to low available B concentration in soils (Shorrocks, 1997). B plays important roles in cell wall formation, membrane integrity, pollen tube growth, sugar transport, nitrogen fixation, plant metabolism and B deficiency leads to nutritional disorders, which inhibit plant apical growth and flower development, and eventually result in decreased plant production (Marschner, 2012). In *Arabidopsis*, B homeostasis is regulated by a synergistic network of several B transporters involved in B uptake, transportation and distribution. Under low B conditions, the transport pathways of B from the *Arabidopsis* root surface to the shoot includes at least three events: (1) NIP5;1, a major boric acid channel, efficiently facilitates B uptake from soil into the root (Takano *et al.*, 2006; Wang *et al.*, 2017); (2) BOR1, a B efflux transporter, is responsible for xylem loading of B (Noguchi *et al.*, 1997; Takano *et al.*, 2002); and (3) NIP6;1 and NIP7;1, homologues of NIP5;1, are required for proper distribution of boric acid in developing shoot tissues and anthers (Routray *et al.*, 2018;

Tanaka *et al.*, 2008). Recently, more B transport-related genes, such as *tassel-less1* (co-orthologue of *AtNIP5;1*) (Matthes *et al.*, 2018) and *rotten ear* (co-orthologue of *AtBOR1*) (Chatterjee *et al.*, 2014) in maize, *OsNIP3;1* (a homologue of *AtNIP5;1*) (Hanaoka *et al.*, 2014; Shao *et al.*, 2018) and *OsBOR1* (a homologue of *AtBOR1*) (Nakagawa *et al.*, 2007) in rice, *VvBOR1* in grapevine (Pérez-Castro *et al.*, 2012), *CmBOR1* in citrus (Cañon *et al.*, 2013) and *TaBOR1s* in wheat (Leaungthitikanchana *et al.*, 2013), have been reported. These studies demonstrated that both boric acid channel NIPs (nodulin 26-like intrinsic proteins) and B transporter BORs are critical for plants to cope with B stress. The B-dependent regulatory mechanism of *AtNIP5;1* was controlled by the 5′ untranslated region (UTR) (Tanaka *et al.*, 2011). To date, transcription factors that regulate B transport-related genes have not been reported in plants. The only reported transcription factor involved in B stress responses was WRKY6 in *Arabidopsis* (Kasajima *et al.*, 2010). Low B induced the promoter activity of *WRKY6* around the root tip, and functional loss of WRKY6 decreased root elongation under both B deficiency and B excess (Kasajima *et al.*, 2010).

Brassica napus (*B. napus*) ($A_nA_nC_nC_n$, 2n = 4x = 38) is extremely sensitive to B deficiency (Marschner, 2012) with typical defect of 'flowering without seed setting' (Xu *et al.*, 2002). In our previous studies, *BnaA3.NIP5;1,* a homologue of *AtNIP5;1*, was identified as a B efficiency candidate gene through quantitative trait locus fine mapping (Hua *et al.*, 2016a). Zhang *et al.* (2017) found that *BnaC4.BOR1;1c*, a homologue of *AtBOR1*, is preferentially expressed in roots, shoot nodes and flower organs and is required for inflorescence development and fertility under low B conditions in *B. napus*. A number of *BnaNIPs* and *BnaBORs,* including *BnaA3.NIP5;1* and *BnaC4.BOR1;1c*, had differential expression in response to varying B availabilities (Hua *et al.*, 2017). Nevertheless, little is known about the molecular regulatory mechanisms underlying low B adaptation of *B. napus*. A comprehensive mRNA transcriptome of *B. napus* suffering from B fluctuation was analysed to identify genome-scale B-responsive genes, and multiple transcription factor families, including the *BnaWRKY* family, were found to be regulated by various B supplies (Hua *et al.*, 2017).

In this study, we carried out a systematic investigation of the involvement of BnaWRKYs in the low B adaptation of *B. napus*. Fifty-one BnaWRKYs responding to B deficiency were identified, and BnaAn.WRKY26, BnaA9.WRKY47, BnaA1.WKRY53 and BnaCn.WRKY57 tested had the binding activity with the conserved W boxes present in the promoters of B transporter genes (*BnaNIP5;1s* and *BnaBOR1s*). Furthermore, BnaA9.WRKY47 was verified to be involved in low B tolerance by specifically activating *BnaA3.NIP5;1* expression through genetic and biochemical approaches. Our study identifies BnaWRKY transcription factors as novel regulators of B deficiency adaptation in *B. napus*.

Results

BnaWRKY family genes respond to B deficiency in *B. napus*

Insufficient B supply impaired growth of *B. napus*, accompanied by curved young leaves and stunted roots (Figure 1a-c). Genome-wide transcriptomic analysis in *B. napus* (Westar 10) has revealed numerous low B-responsive genes, including transcription factors, signal transducers and structural molecules (Hua *et al.*, 2017). Among these responsive genes, 51 *WRKY* transcription factor family genes showed more than twofold differential expression under B deficiency (0.25 μM B) relative to the normal B condition (25 μM B) (Figure 1d and Table S1). Of these, 16 *BnaWRKYs* were up-regulated and 5 genes were down-regulated in roots, while 32 *BnaWRKYs* were up-regulated and 3 genes were down-regulated in shoots (Figure 1e). Notably, 4 *BnaWRKYs* were induced and 1 *BnaWRKY* was reduced in both roots and shoots by low B. qRT-PCR analyses of random 10 B-responsive WRKY genes (Figure S1) confirmed the differential expression in response to low B stress and showed a high correlation with the expression from RNA-Seq (R^2 = 0.9415) (Figure 1f).

BnaWRKYs bind to the conserved *cis*-element present in the promoter regions of B transport-related genes

A conserved W box (T/CTGACC/T) in the promoter region of target genes was identified as the typical binding site of WRKY (Eulgem *et al.*, 2000). The boric acid channel AtNIP5;1 for B uptake and transporter AtBOR1 for B xylem loading are pivotal for the efficient transcellular transport of B under B limited conditions (Miwa and Fujiwara, 2010). Interestingly, the differential expression of the homologues of *NIP5;1s* and *BOR1s* in *B. napus* under B deficiency appeared to be correlated with the W-box sequences present in their promoter regions. Among six *BnaNIP5;1s, BnaA2.NIP5;1*, *BnaA3.NIP5;1* (Hua *et al.*, 2016a), *BnaC2.NIP5;1* and *BnaC3.NIP5;1* were obviously up-regulated in roots under B deficiency (Figure 2a). It was interesting that these four *BnaNIP5;1s* and *AtNIP5;1* contain a 16-bp conserved sequence ($W^{C\text{-}N}$ in Figure 2a) with a W box (TTGACT) in their promoters, whereas *BnaA7.NIP5;1* and *BnaC6.NIP5;1,* whose expression was less affected by low B, do not have the conserved $W^{C\text{-}N}$ (Figure 2a). Similarly, a 17-bp conserved sequence ($W^{C\text{-}B}$) with a W box (TTGACT/C) was found in *AtBOR1* and four *BnaBOR1s,* including *BnaA3.BOR1;3a*, *BnaA4.BOR1;1a*, *BnaA5.BOR1;2a* and *BnaC4.BOR1;2c*, which were induced by low B with the exception of *BnaA3.BOR1;3a* (Figure 2b). Thus, we presumed that BnaWRKYs participate in low B stress by regulating the expression of boric acid channel and B transporters.

To verify this possibility, yeast one-hybrid (Y1H) assays were performed. Based on the DEGs (Figure 1) and co-expression network analysis (Figure S2), *BnaAn.WRKY26, BnaA9.WRKY47, BnaA1.WRKY53* and *BnaCn.WRKY57* were selected for prey construct using the pGADT7-Rec2 vector. Four tandem copies of conserved W-box sequences ($4 \times W^{C\text{-}N}$ and $4 \times W^{C\text{-}B}$) were cloned into the pHIS2 reporter vector and used as baits for the binding assays (Figure 2c). All the yeasts could grow well on selective dropout medium (SD/-Leu-Trp-His) without 3-AT (3-amino-1, 2,4-triazole). When 50 mM 3-AT was added, the positive control (pGADT7-53 and pHIS2-53) grew normally, while the negative control (pGADT7-53 and pHIS2 empty vector) could not survive. It was evident that all the $4 \times W^{C\text{-}N}$-WRKY or $4 \times W^{C\text{-}B}$-WRKY co-transformants were able to grow on the 3-AT containing selective dropout medium (Figure 2d,e), indicating the potential for interaction between BnaWRKYs and *BnaNIP5;1s*, or BnaWRKYs and *BnaBOR1s*.

BnaA9.WRKY47 is a nuclear-localized transcription factor

To elucidate the molecular mechanism of *BnaWRKYs* functioning in low B adaptation of *B. napus*, *BnaA9.WRKY47* was selected to be further analysed owing to its significant up-regulation by B deficiency in both roots and leaves and relatively higher mRNA expression abundance than other *BnaWRKY* DEGs (Figures 1d, 3a, 3b and S1). By transient expression of *35S*:BnaA9.WRKY47:GFP (green fluorescent protein) in *Arabidopsis* protoplasts, the GFP signal was exclusively co-localized with the CFP (cyan

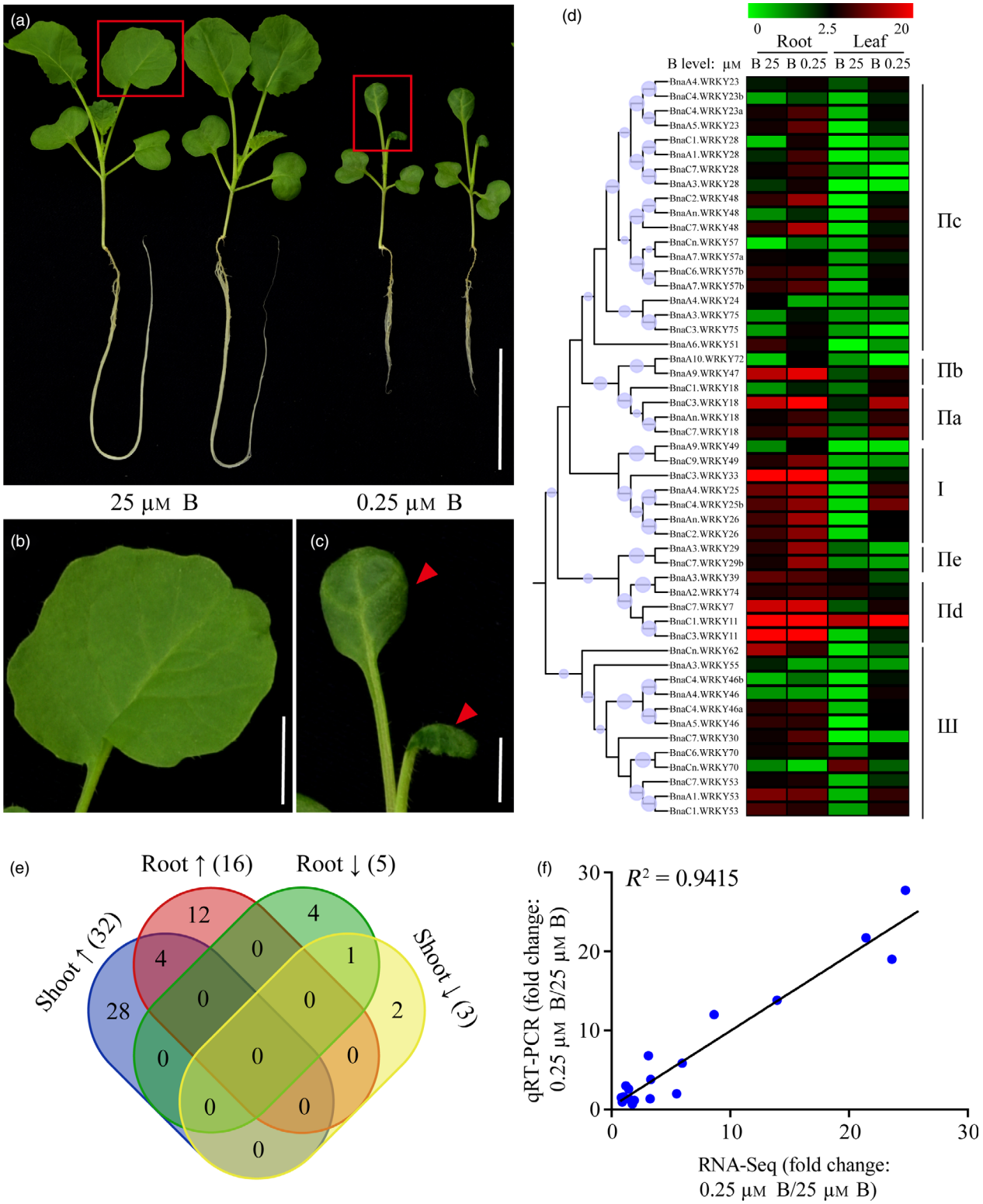

Figure 1 Low B stress induces differential expression of *BnaWRKY* family genes. (a) The phenotype of *B. napus* 'Westar 10' seedlings grown under B sufficiency (25 μM B) and B deficiency (0.25 μM B) conditions for 10 days. Bar = 5 cm. (b–c) Close-up view of leaves indicated by red squares in (a). Bars = 1 cm. (d) Heat map of 51 *BnaWRKY* genes with differential expression in response to low B stress. (e) Venn diagram of the 51 *BnaWRKY* DEGs in roots and shoots. The upward and downward arrows indicate up-regulated and down-regulated genes, respectively. The number of DEGs in the Venn graph represents the *BnaWRKY* quantity. (f) Correlation of expression ratios between qRT-PCR and RNA-Seq for 10 *BnaWRKY* genes. [Colour figure can be viewed at wileyonlinelibrary.com]

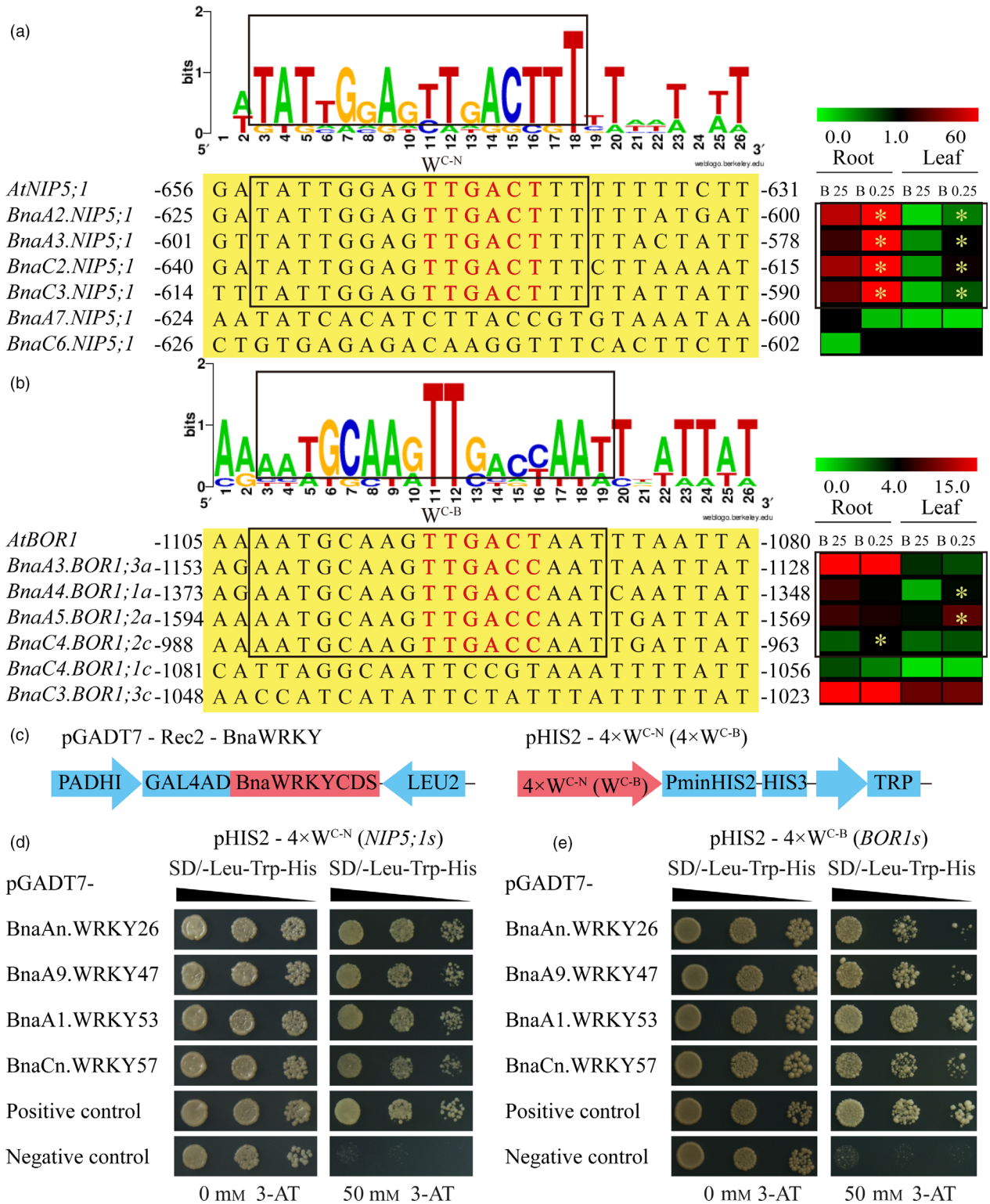

Figure 2 BnaWRKYs interact with *BnaNIP5;1s* and *BnaBOR1s* in yeast. (a-b) Multiple sequence alignment of promoter and gene expression profiling of *BnaNIP5;1s* (a) and *BnaBOR1s* (b). Conserved sequences in the promoters of *BnaNIP5;1s* and *BnaBOR1s* are indicated by '$W^{C\text{-}N}$' and '$W^{C\text{-}B}$', respectively. W-box sequences are highlighted in red. The significantly differentially expressed *BnaNIP5;1s* and *BnaBOR1s* genes are labelled by asterisks in the heatmaps. (c–e) Yeast one-hybrid assays of binding activity of BnaWRKYs with conserved *cis*-elements of the promoters of *BnaNIP5;1s* (d) and *BnaBOR1s* (e). Yeast cells were cotransformed with pGADT7-BnaWRKYs and pHIS2-*cis* (4 × $W^{C\text{-}N}$ or 4 × $W^{C\text{-}B}$), then grown on selective dropout medium (SD/-Trp-Leu-His) containing 0 or 50 mM 3-AT. 'pHIS2-53/pHIS2 plus pGADT7-53' were the positive and the negative controls, respectively. [Colour figure can be viewed at wileyonlinelibrary.com]

fluorescent protein)-labelled Ghd7 nuclear signal (Figure 3c) demonstrating that BnaA9.WRKY47 was localized in the nucleus.

BnaA9.WRKY47 positively regulates low B adaptation of *B. napus*

To investigate whether BnaA9.WRKY47 plays an important role in low B adaptation of *B. napus,* homozygous CRISPR/Cas9 mediated mutants possessing three editing types in the genome region of the *BnaA9.WRKY47* gene (CR#19 carried a 2-bp deletion and a 1-bp insertion; CR#24 carried a 1-bp deletion and a 1-bp insertion; and CR#88 carried a 2-bp deletion, a 1-bp insertion and a 16-bp mutation) (Figure 4a) and three independent overexpressing lines (OE#177, OE#184 and OE#385) with 10- to 30-fold elevated expression levels compared with wide-type 'Westar 10' (Figure 4b) were established. No distinguishable differences in phenotype were observed in all lines when grown in the 25 μM B condition (Figure 4c). In 0.25 μM B, all three gene-edited mutants displayed stronger growth inhibition in both leaves and roots compared with wild-type plants; conversely, overexpressing lines showed dramatic tolerance to low B compared with the wild-type plants (Figure 4c). The phenotypic differences among all genetic lines were further supported by the dry weights of both shoots and roots (Figure 4d,e). The B contents of the gene-edited mutants and overexpressing lines were significantly lower and higher, respectively, than in wild-type plants in both shoots and roots under the 0.25 μM B treatment (Figure 4f,g). However, the phenotype, dry weight and the B contents were indistinguishable among wild-type plants, mutants and overexpressing lines under sufficient B supply (25 μM) (Figure 4). Juvenile leaves and root tips are the most sensitive tissues in response to low B stress. In 25 μM B, all lines developed fully expanded new leaves, but 0.25 μM B treatment led to deformed and curly juvenile leaves; the degree of curliness of juvenile leaves was further aggravated in the gene-edited lines and was largely alleviated in the overexpressing lines (Figure 5a), which was reflected by new leaf areas (Figure 5b). Consistent with the phenotypic characterization, all lines had comparable B concentrations in juvenile leaves at 25 μM B, but at 0.25 μM B, the gene-edited lines had lower B concentrations and the overexpressing lines had higher B

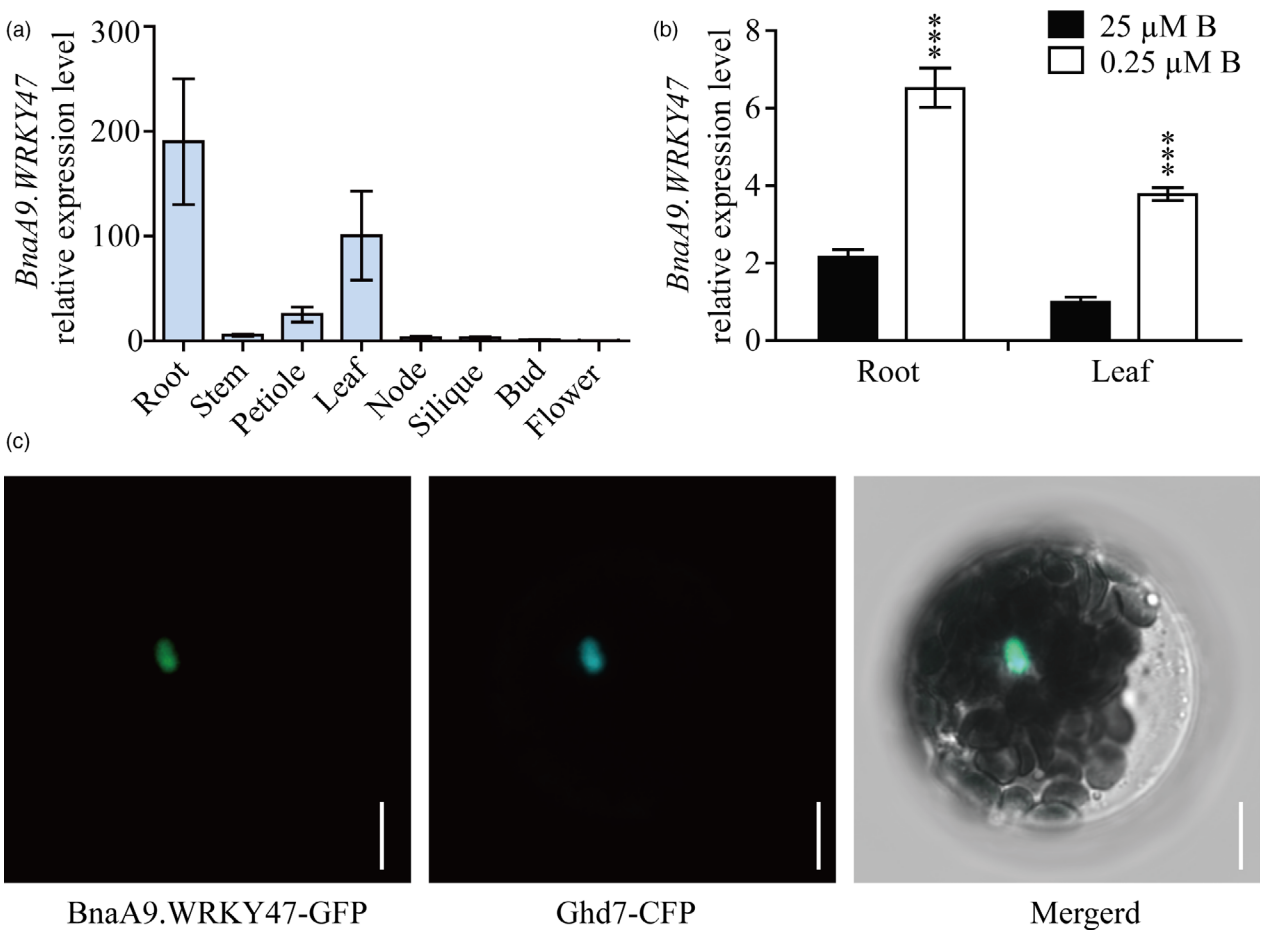

Figure 3 *BnaA9.WRKY47* is up-regulated in roots and leaves under B limitation and is a nuclear-localized transcription factor. (a) qRT-PCR analysis of *BnaA9.WRKY47* expression in various tissues of 'Westar 10' at the flowering stage supplied with 9 kg borax/ha. *BnaEF1α* and *BnaTubulin* mRNAs were used as internal controls. Data are shown as the means ± SD (n = 3). (b) qRT-PCR analysis of *BnaA9.WRKY47* expression in 'Westar 10' under B sufficiency and B deficiency. Seven-day-old 'Westar 10' seedlings were transferred to nutrient solution containing 25 μM or 0.25 μM boric acid. *BnaEF1α* and *BnaTubulin* mRNAs were used as internal controls. Data are shown as the means ± SD (n = 3). Asterisks indicate significant differences compared with B sufficiency (t-test, *** $P < 0.001$) (c) Subcellular localization of the BnaA9.WRKY47:GFP fusion protein in *Arabidopsis* protoplasts. Bars = 20 μm. [Colour figure can be viewed at wileyonlinelibrary.com]

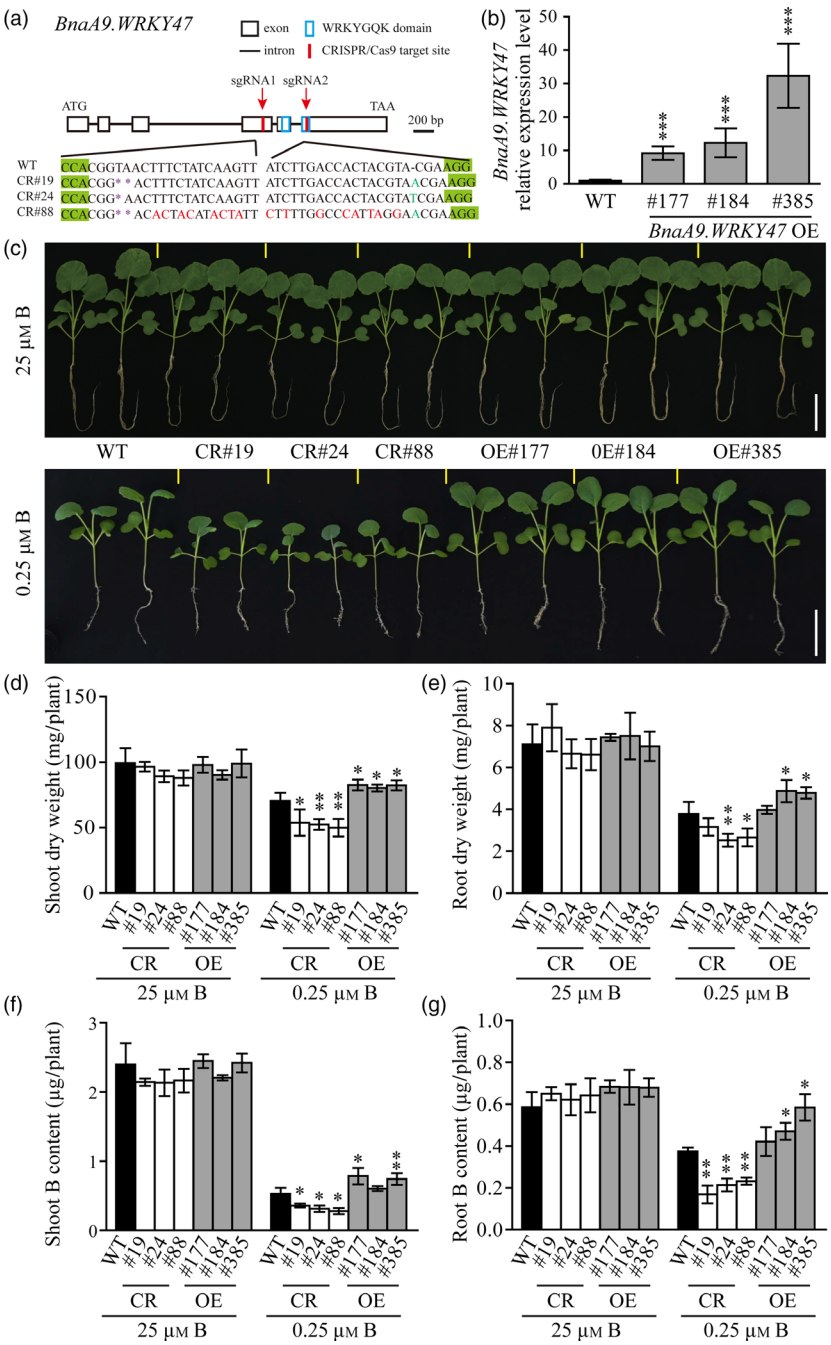

Figure 4 *BnaA9.WRKY47* positively regulates low B adaptation of *B. napus*. (a) CRISPR/Cas9-mediated target mutagenesis of *BnaA9.WRKY47* (CR). The edit types of three *BnaA9.WRKY47* homozygous mutants (CR#19, 24, 88) are shown. (b) Overexpressing line (OE) establishment by qRT-PCR analysis of *BnaA9.WRKY47* expression. Leaf samples were detached from 17-day-old plants grown under 25 μM boric acid. *BnaEF1α* and *BnaTubulin* mRNAs were used as internal controls. Mean values ± SD are shown (n = 3). Asterisks indicate significant differences compared with wild-type plants (t-test, *** $P < 0.001$). (c) Photographs of all lines grown under 25 μM B and 0.25 μM B conditions for 15 days. Bars = 5 cm. (d-e) The shoot (d) and root (e) dry weights of various plant materials grown for 15 days under 25 μM B and 0.25 μM B were calculated. Mean values ± SD are shown (n = 5). Asterisks indicate significant differences compared with wild-type plants (t-test, * $P < 0.05$, ** $P < 0.01$). (f–g) The shoot and root B contents of various plant materials grown for 15 days under 25 μM B and 0.25 μM B were calculated. Mean values ± SD are shown with four biological replicates and two plants per replicate. Asterisks indicate significant differences compared with wild-type plants (t-test, * $P < 0.05$, ** $P < 0.01$). [Colour figure can be viewed at wileyonlinelibrary.com]

concentrations than wild type (Figure 5c). B deficiency also impaired root morphology and caused tip necrosis (Figure S3). Malondialdehyde (MDA) is a product of lipid peroxidation (Bejaoui *et al.*, 2016), and the degree of tissue damage by low B can be reflected by MDA concentration to a certain extent (Hua *et al.*, 2016b). Under the 25 μM B condition, all tested plants showed no obvious differences in root MDA concentration. However, under the 0.25 μM B condition, the overexpressing lines had the lowest root MDA concentrations followed by the wild-type 'Westar 10', and the mutants had highest (Figure 5d); and the lower the MDA concentration was, the higher the B concentration that was detected in roots (Figure 5e).

BnaA9.WRKY47 positively regulates *BnaA3.NIP5;1* transcription

We thus investigated the transcription levels of *BnaNIP5;1s* and *BnaBOR1s* in *BnaA9.WRKY47* null mutants and overexpressing lines to test whether BnaA9.WRKY47-mediated low B adaptation is dependent on B transport-related genes. The expressions of *BnaA2.NIP5;1* and *BnaC2.NIP5;1* were decreased in the new leaves of *BnaA9.WRKY47* CR#24 mutants but increased in *BnaA9.WRKY47* overexpressing line OE#184 with low B; however, no obvious differences were observed in the roots of various lines (Figure 6a,b). There was no significant difference in the expression of *BnaC3.NIP5;1* in *BnaA9.WRKY47* transgenic lines

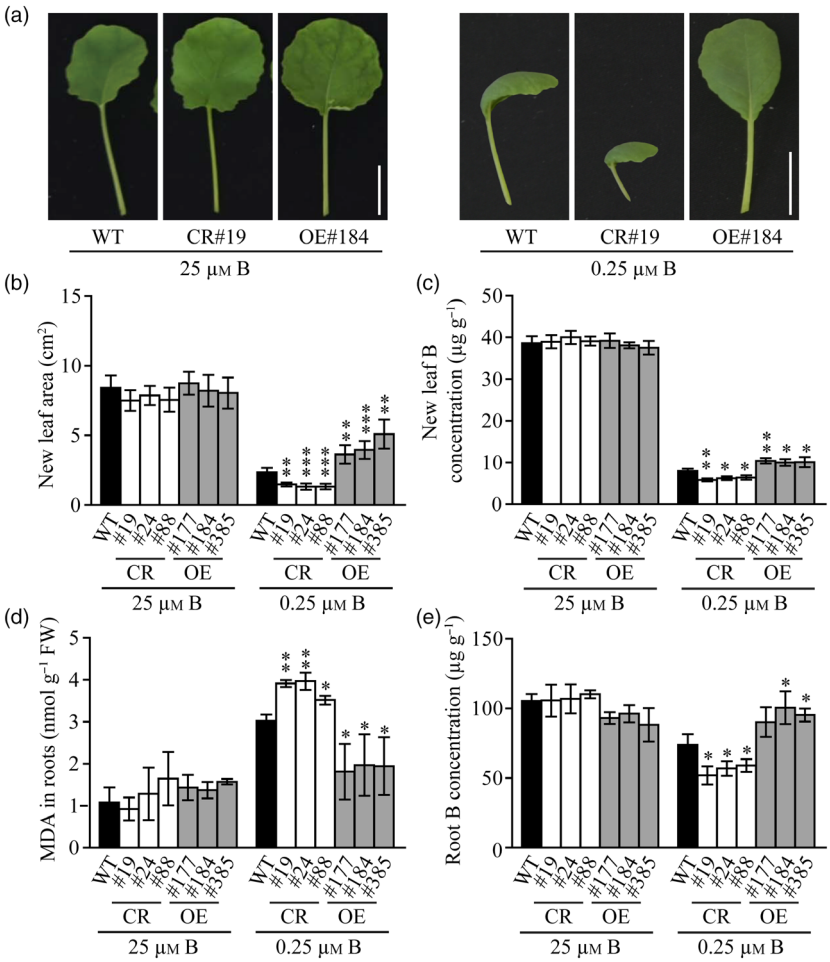

Figure 5 *BnaA9.WRKY47* affects the growth of new leaves and roots under low B treatment. (a) Photographs of the new leaves of 'Westar 10' and transgenic lines grown under 25 μM B and 0.25 μM B conditions for 15 days. Bars = 2 cm. (b) Statistical analysis of new leaf size of plants grown hydroponically under 25 μM B and 0.25 μM B conditions for 15 days. Mean values ± SD are shown (n = 5). Asterisks indicate significant differences compared with wild-type plants (t-test, ** $P < 0.01$, *** $P < 0.001$). (c) New leaf B concentration measurement of the all lines grown hydroponically under 25 μM B and 0.25 μM B conditions for 15 days. Mean values ± SD are shown (n = 4). Asterisks indicate significant differences compared with wild-type plants (t-test, * $P < 0.05$, ** $P < 0.01$). (d) Statistical analysis of MDA concentrations in roots. Root samples were detached from various lines grown under 25 μM B and 0.25 μM B conditions for 15 days. Mean values ± SD are shown, with three biological replicates and two plants per replicate. Asterisks indicate significant differences compared with wild-type plants (t-test, * $P < 0.05$, ** $P < 0.01$). (e) Root B concentration measurements of the all lines grown hydroponically under 25 μM B and 0.25 μM B conditions for 15 days. Mean values ± SD are shown (n = 4). Asterisks indicate significant differences compared with wild-type plants (t-test, * $P < 0.05$). [Colour figure can be viewed at wileyonlinelibrary.com]

(Figure 6a,b), and *BnaA7.NIP5;1* and *BnaC6.NIP5;1* mRNA abundance was barely detected under our experimental conditions. Noticeably, under B sufficiency, there were no obvious differences in *BnaA3.NIP5;1* expression among the wild-type and various transgenic plants, whereas the expression of *BnaA3.NIP5;1* in new leaves and roots was reduced in *BnaA9.WRKY47* mutants but significantly induced in overexpressing lines under B deficiency (Figure 6a,b). Moreover, there was no significant difference in the expression of *BnaBOR1s*, except for *BnaA3.BOR1;3a* that was reduced in both *BnaA9.WRKY47* mutants and overexpressing lines, between *BnaA9.WRKY47* transgenic plants and wild-type under both B deficiency and B sufficiency (Figure S4). These data suggest that the boric acid channel gene *BnaA3.NIP5;1* might be the target gene, downstream of BnaA9.WRKY47.

Subsequently, a 3176-bp fragment upstream of the *BnaA3.NIP5;1* start codon was isolated from 'Westar 10'. In addition to the conserved $W^{C\text{-}N}$ sequence, we found that *BnaA3.NIP5;1* had another four W-box core elements (TGAC), whose location relative to the transcription start site (+1) are −1559 to −1556, −735 to −732, −661 to −658 and −646 to −643 (Figure 6c). To verify the transcriptional regulation of *BnaA3.NIP5;1* by BnaA9.WRKY47, the sequence W^{S}, −669 to −641 plus −601 to −582, which contains two TGAC core sequence and the conserved W-box domain ($W^{C\text{-}N}$) (Figure 6c), was cloned into the pHIS2 vector for Y1H assays. All transformed yeasts grow well on selective medium without 3-AT. The transformants of the pHIS2-W^{S} plus pGADT7-BnaA9.WRKY47 and the positive control could grow well, but the negative control was completely inhibited on selective media with 50 mM 3-AT (Figure 6d). In order to understand the effect of the three TGAC elements on the interaction of BnaA9.WRKY47 with *BnaA3.NIP5;1*, the Y1H assays were conducted further with the transformants of single/double/triple mutation in TGAC sequences of W^{S} (Figure S5a).

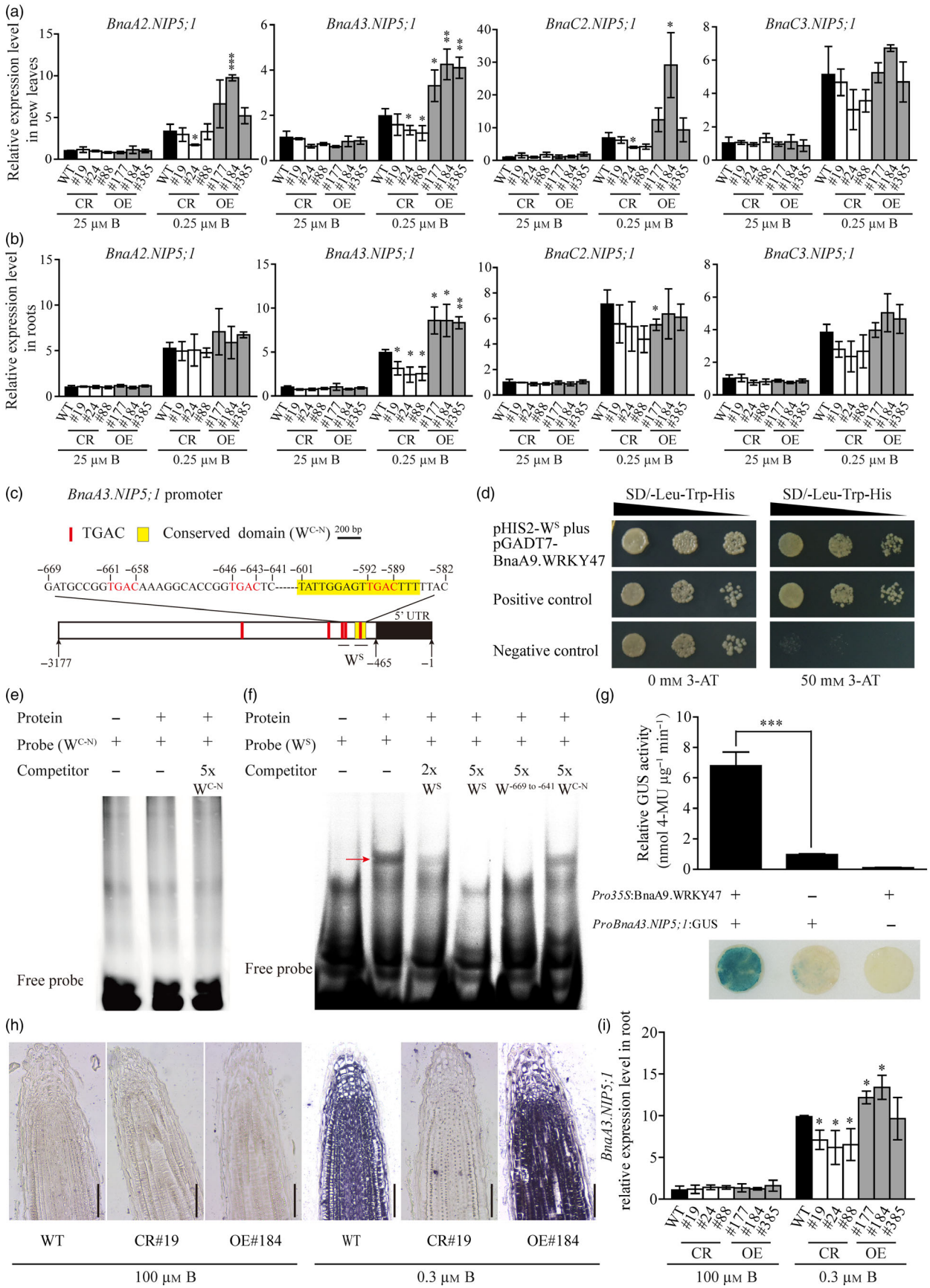

Figure 6 BnaA9.WRKY47 directly activates the expression of *BnaA3.NIP5;1*. (a-b) qRT-PCR analysis of *BnaNIP5;1s* expression in the new leaves and roots of the wild-type 'Westar 10', *BnaA9.WRKY47* mutants and overexpressing plants. Gene expression was normalized by *BnaEF1α* and *BnaTubulin* mRNAs with three biological replicates. Asterisks indicate significant differences in gene expression levels between *BnaA9.WRKY47* transgenic lines and 'Westar 10' (*t*-test, * $P < 0.05$, ** $P < 0.01$, *** $P < 0.001$). (c) Characterization of the *BnaA3.NIP5;1* promoter sequence. The TGAC core sequence and conserved sequence $W^{C\text{-}N}$ of *BnaNIP5;1s* were marked by a red and yellow rectangle, respectively. The specific sequence W^{S} of *BnaA3.NIP5;1* was shown. (d) The interaction of BnaA9.WRKY47 protein with *BnaA3.NIP5;1*-specific promoter region (W^{S}) in yeast. (e-f) Electrophoretic mobility shift assay to analyse the interaction of BnaA9.WRKY47 and the conserved $W^{C\text{-}N}$ in *BnaNIP5;1s* (e) or the specific W^{S} (f) in the *BnaA3.NIP5;1* promoter. The 5′ Cy5 labelled probe was incubated with BnaA9.WRKY47-His protein at 25°C for 20 min. Competition for the labelled sequences was tested by adding different concentrations of unlabelled probes. The binding shift is indicated with a red arrow. (g) Transient expression assay of *BnaA3.NIP5;1* activated by BnaA9.WRKY47 in tobacco leaves. GUS activities were detected after *35S:BnaA9.WRKY47* and *proBnaA3.NIP5;1:GUS* were injected into tobacco leaves together or separately for 2 days. Values represent mean values ± SD of three biological replicates, and two independent experiments verified these results. Asterisks indicate significant differences based on a *t*-test (*** $P < 0.001$). (h) In situ hybridization analysis of *BnaA3.NIP5;1* expression in the root tips of *BnaA9.WRKY47* transgenic plants. Longitudinal sections of the root tips from wild-type, CR#19 and OE#184 seedlings grown on solid medium containing 100 μM B or 0.3 μM B for 5 days. The root tips were hybridized with *BnaA3.NIP5;1*-specific antisense probe labelled with DIG. Bars = 100 μm. (i) qRT-PCR analysis of *BnaA3.NIP5;1* expression in the roots of the *BnaA9.WRKY47* transgenic plants grown on solid medium containing 100 μM B or 0.3 μM B for 5 days. Gene expression was normalized by *BnaEF1α* and *BnaTubulin* mRNAs with three biological replicates. Asterisks indicate significant differences in gene expression levels between *BnaA9.WRKY47* transgenic lines and 'Westar 10' (*t*-test, * $P < 0.05$). [Colour figure can be viewed at wileyonlinelibrary.com]

The yeast growth of the wild type (W^{S}) and all the transformants was indistinguishable at 50 mM 3-AT, while mW^{2}, mW^{12}, mW^{13}, mW^{23} and mW^{123} were visibly inhibited at 100 mM 3-AT. When 3-AT concentration was increased to 150 mM, the inhibition effect was more serious in mW^{2}, mW^{12}, mW^{23} and mW^{123} compared with W^{S} (Figure S5b). These results suggest that the BnaA9.WRKY47 protein could bind with the promoter region of *BnaA3.NIP5;1* in yeast, and at least the box element $TGAC^{-646\ to\ -643}$ could effectively affect the binding activity of BnaA9.WRKY47 to *BnaA3.NIP5;1*.

An electrophoretic mobility shift assay (EMSA) was performed to confirm whether the BnaA9.WRKY47 protein could bind directly to the promoter of *BnaA3.NIP5;1* in vitro. The conserved $W^{C\text{-}N}$ sequence in *BnaNIP5;1s* and the specific W^{S} sequence in the *BnaA3.NIP5;1* promoter were synthesized as probes and incubated with the BnaA9.WRKY47 protein generated in *Escherichia coli*. It was evident that BnaA9.WRKY47 could not bind with the conserved $W^{C\text{-}N}$ (Figure 6e) but obviously interacted with the specific W^{S} probe, and excess W^{S} unlabelled probes (twofold and fivefold) could competitively inhibit the combination (Figure 6f). Moreover, the binding of W^{S} with BnaA9.WRKY47 was completely inhibited by fivefold unlabelled −669 to −641 sequence (referred to $W^{-669\ to\ -641}$), but the shift binding rates were less affected by the addition of unlabelled $W^{C\text{-}N}$ (Figure 6f). The mutation either in C^{-658} or in C^{-589} did not weaken the binding of probes with BnaA9.WRKY47, while mutation in C^{-643} greatly impaired the affinity of probe to BnaA9.WRKY47 in EMSA (Figure S6b). Together with the Y1H assay, these results indicated that the W-box element $TGAC^{-646\ to\ -643}$ presumably played an important role in the binding of BnaA9.WRKY47 with *BnaA3.NIP5;1*.

To further investigate whether BnaA9.WRKY47 could activate *BnaA3.NIP5;1* expression, a transient expression assay was performed in tobacco leaves. The *proBnaA3.NIP5;1*:GUS vector was co-expressed with or without *35S*:BnaA9.WRKY47 in tobacco (*Nicotiana benthamiana*) leaves. The GUS activity and GUS staining results showed that *proBnaA3.NIP5;1*:GUS alone was barely expressed in tobacco leaves but the expression was elevated by about sevenfold when it was co-injected with *35S*:BnaA9.WRKY47 (Figure 6g), indicating that BnaA9.WRKY47 significantly activated the expression of *BnaA3.NIP5;1*.

We further carried out RNA in situ hybridization to detect *BnaA3.NIP5;1* expression in *BnaA9.WRKY47* transgenic lines and wild type. As a boric acid channel, NIP5;1 mainly functions in root tips for efficient B uptake. In longitudinal sections of root tips, the hybridization signal of *BnaA3.NIP5;1* was barely detected in wild-type, *BnaA9.WRKY47* knockout mutants and overexpressing lines under high-B condition (100 μM B). Under low B condition (0.3 μM B), the antisense probe of *BnaA3.NIP5;1* showed obvious hybridization signal in the root tip of wild-type, but only a background signal level in the *BnaA9.WRKY47* knockout line (CR#19). In contrast, stronger hybridization signal was detected in *BnaA9.WRKY47* overexpressing line (OE#184) compared with wild-type (Figure 6h). Consistent with the in situ hybridization results in root tips, the qRT-PCR analyses indicate that there were no significant differences in *BnaA3.NIP5;1* expression in the roots among *BnaA9.WRKY47* transgenic lines and wild-type under high-B condition, but significantly lower and higher expressions of *BnaA3.NIP5;1* under low B treatment were detected in *BnaA9.WRKY47* mutants and overexpressing lines compared with wild-type, respectively (Figure 6i).

Discussion

BnaWRKYs act as new players in response of *B. napus* to B deficiency

Plants can sense and cope with stressful environments depending on various transcription factor-mediated stress adaptation (Chinnusamy *et al.*, 2004). The WRKY transcription factor family is one of the most important regulator families responding to nutrition disorders in plants. For example, an increasing number of studies have identified multiple WRKYs that modulate Pi homeostasis in plants (Devaiah *et al.*, 2007; Chen *et al.*, 2009; Wang *et al.*, 2014; Dai *et al.*, 2016; Su *et al.*, 2015). To date, the only WRKY described as a regulator of B stress is AtWRKY6 (Kasajima *et al.*, 2010). Our understanding of WRKY functioning in low B remains limited. In the present study, fifty-one of 287 *BnaWRKYs* (He *et al.*, 2016) were detected as B-responsive DEGs (Figure 1 and Table S1). Among them, 44 DEGs (86%) and 7 DEGs (14%) exhibited elevated and decreased mRNA abundance with low B treatment, respectively. Up-regulated DEGs were predominant in both leaves (91%) and roots (76%). It is possible that BnaWRKY proteins mainly act as positive regulators under low B. There are fewer DEGs that up-regulated or down-regulated simultaneously in the leaves (four) and roots (one), this finding may reflect the functional differentiation and tissue specificity of BnaWRKYs. The B transporter-related genes (*NIP5;1*, *NIP6;1*, *NIP7;1*, *BOR1*, *BOR2*,

BOR4) have abundant W boxes in their 2000 bp promoter sequences (Table S2), implying that BnaWRKY transcription factors might interact with B transporter genes. The binding of BnaWRKYs to the conserved W boxes of B-responsive *BnaNIP5;1s* and *BnaBOR1s* in Y1H assays (Figure 2d,e) suggests that BnaWRKYs might participate in B stress adaptation by modulating *BnaNIP5;1s* and/or *BnaBOR1s*. Furthermore, the *BnaA9.WRKY47* mutants displayed severe B deficiency phenotypes under B deficiency and the *BnaA9.WRKY47* overexpressing lines showed higher tolerance of low B than wild-type 'Westar 10' (Figure 4 and 5), indicating that BnaWRKYs act as new players in the response of *B. napus* to B deficiency, although further investigation is required to support this conclusion.

BnaA9.WRKY47-BnaA3.NIP5;1 cascade modulates low B adaptation of *B. napus*

The B deficiency phenotype in new leaves and roots of *BnaA9.WRKY47* mutants under low B conditions disappeared in the *BnaA9.WRKY47* overexpressing lines (Figure 4c), suggesting enhanced BnaA9.WRKY47 activity facilitates B accumulation in *B. napus*. As expected, the B concentrations were higher in these *BnaA9.WRKY47* overexpressing lines than in wild-type 'Westar 10' and *BnaA9.WRKY47* null mutants (Figure 4f,g). Interestingly, a boric acid channel gene *BnaA3.NIP5;1* was significantly up-regulated and down-regulated in the *BnaA9.WRKY47* overexpressing lines and its null mutants, respectively (Figure 6a,b), but the expression of other *BnaNIP5;1s* and *BnaBOR1s* was less affected in *BnaA9.WRKY47* transgenic lines (Figure 6a,b and S4). Although BnaA9.WRKY47 showed binding activity with conserved W-box *cis*-elements in the promoters of several *BnaNIP5;1s* and *BnaBOR1s* (Figure 2d,e), it is reasonable that BnaA9.WRKY47 specifically activates *BnaA3.NIP5;1* expression by 'TGAC'-containing sequence repeats rather than the conserved W box in the EMSA assays (Figure 6e,f and Figure S6); adjacent sequences of W boxes also partly determine binding site preference leading to specificity for their target promoters (Ciolkowski *et al.*, 2008). *BnaA3.NIP5;1* was identified in our previous work as a key candidate gene for the determinant of B efficiency in different low B-sensitive *B. napus* cultivars (Hua *et al.*, 2016a). The B efficient cultivar 'Qingyou 10' and the near-isogenic lines containing the *BnaA3.NIP5;1* gene of 'Qingyou 10' with 'Westar 10' background have higher expression levels of *BnaA3.NIP5;1* and stronger low B tolerance than B-inefficient 'Westar 10' (Hua *et al.*, 2016a). In *Arabidopsis*, the upstream open reading frame (uORF), AUG-stop in the 5′ untranslated region of the *AtNIP5;1* promoter induces B-dependent mRNA degradation (Tanaka *et al.*, 2011, 2016). However, the BnaA9.WRKY47 activation of *BnaA3.NIP5;1* expression might be an uORF-independent mechanism because the BnaA9.WRKY47 target *cis*-elements are not in the 5′ UTR of *BnaA3.NIP5;1* (Figure 6c) and no uORFs were changed in both 'QY10' and 'Westar 10' (Hua *et al.*, 2016a). The activation of *BnaA3.NIP5;1* by BnaA9.WRKY47 in *Nicotiana tabacum* cells and in situ hybridization (Figure 6g,h), and the nuclear localization of BnaA9.WRKY47 (Figure 3c) suggested that BnaA9.WRKY47 truly activates *BnaA3.NIP5;1* expression in the nuclei of *B. napus*. Taken together, the BnaA9.WRKY47 transcription factor and boric acid channel gene *BnaA3.NIP5;1* form a cascade that modulates low B adaptation in *B. napus*.

In conclusion, we propose a working model to illustrate the involvement of *BnaWRKYs* in the response to low B stress (Figure 7). When *B. napus* suffers from low B stress, the dynamic web of 51 BnaWRKY DEGs regulate transcriptional reprogramming associated with adaptation to low B, and BnaWRKYs act as

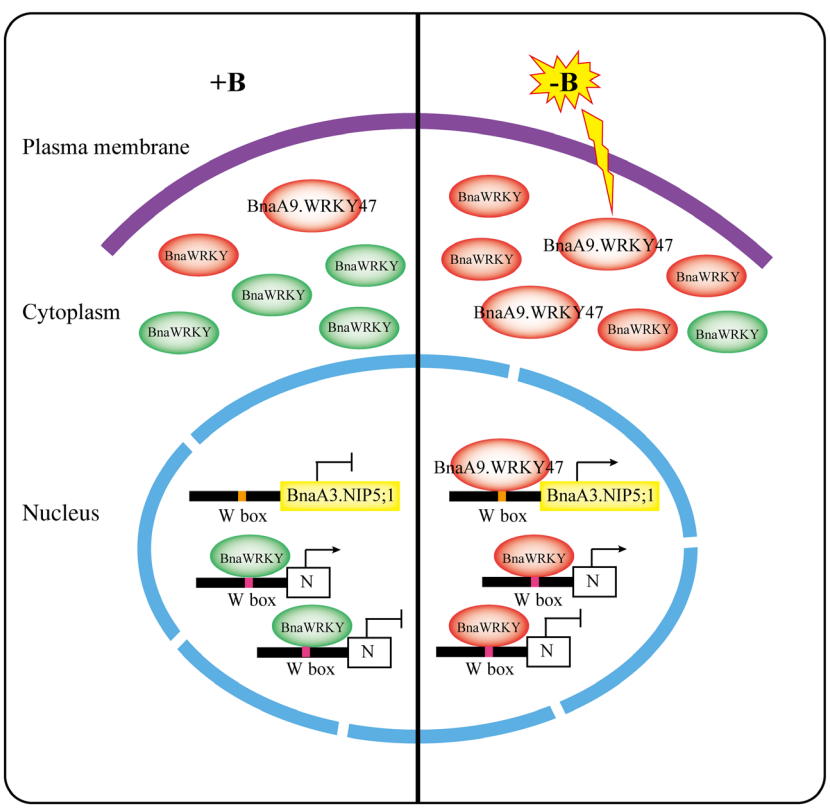

Figure 7 A conceptual framework illustrating how the BnaA9.WRKY47-BnaA3.NIP5;1 cascade modulates low B adaptation of *B. napus*. *BnaWRKY* family genes, including *BnaA9.WRKY47,* are regulated by low B stress, the ellipses coloured red and green indicate *BnaWRKYs* that are up-regulated and down-regulated by low B, respectively. Under B sufficiency, *BnaA3.NIP5;1* was repressed, under B deficiency, the elevated *BnaA9.WRKY47* specifically activated the expression of boric acid channel gene *BnaA3.NIP5;1* by binding to the W-box elements. Increased expression of BnaA3.NIP5;1 facilitates B uptake for plant growth. In addition, other low B-responsive BnaWRKYs may function as activators or repressors in low B adaptation by regulating unknown target genes (N). [Colour figure can be viewed at wileyonlinelibrary.com]

repressors and activators. Among these BnaWRKYs, the up-regulated *BnaA9.WRKY47,* in particular, activates the expression of the boric acid channel gene *BnaA3.NIP5;1* and improves the adaptation to low B of *B. napus*. More BnaWRKYs may be critical factors in B nutrition through the same or different pathways as BnaA9.WRKY47, which needs to be studied further.

Experimental procedures

Plant materials and growth conditions

The *B. napus* cultivar 'Westar 10' stored in this laboratory was used to perform the analyses of the phenotype and mRNA expression profiling. Plump seeds with similar size were surface-sterilized for 15 min using 1% NaClO and washed with ultrapure water (18.25 MΩ·cm). Then, these seeds were sown on a piece of gauze moistened with ultrapure water. After germination for 7 days, uniformly sized seedlings were transferred to Hoagland solution (Hoagland and Arnon, 1950) (HS) with B deficient (0.25 μM B) or B sufficient (25 μM B) treatments for 10–15 days. The nutrient solution was refreshed every three days with gradually increasing nutrient strength, including 1/4 HS for 3 days, 1/2 HS for 3 days and complete HS for 4–9 days. The plants were cultivated in an illuminated growth room under 16-h-light/8-h-dark photoperiod (with a photon flux density of 300-320 μmol m^{-2} s^{-1} and a relative humidity of 60%). Leaves and roots were harvested with three to five biological replicates for transcriptome sequencing, qRT-PCR and B concentration detection. Pictures were taken by a digital camera (Nikon, Tokyo, Japan) or stereoscopic microscope (Olympus, Tokyo, Japan).

Identification of differential expression genes (DEGs)

Transcriptome sequencing was performed as described (Hua *et al.*, 2017). A basic local alignment search tool (BLASTn) program was performed between *Arabidopsis* Information Resource (TAIR 10) (https://www.arabidopsis.org/) and *Brassica* Database (BRAD) (http://brassicadb.org/brad/index.php) to identify the homologues in the allotetraploid *B. napus* genome. FDR (false discovery rate) ≤ 0.05 and the fold-change ≥ 2 were used as the threshold to screen the differentially expression genes (Audic and Claverie, 1997). Heat maps of DEGs were delineated by Multiexperiment Viewer, and a phylogenetic tree of DEGs was constructed by MEGA 6.0.

Sequence analysis

The genome sequences and amino acid sequences of *B. napus* 'Westar 10' were obtained from the *Brassica* Database (Chalhoub *et al.*, 2014; Cheng *et al.*, 2011), and the sequences of *Arabidopsis* were downloaded from TAIR 10 database (Reiser *et al.*, 2017). The 2000 bp upstream sequences from the start codons of *BnaWRKY* genes and B-related genes were analysed to determine the *cis*-regulatory elements (W box).

Quantification of gene expression

Total RNA was extracted using the EastepR Super Total RNA Extraction Kit (Promega, Madison, WI). The first-strand cDNA was reverse transcribed by ReverTra Ace qPCR RT Master Mix with gDNA Remover (TOYOBO, Osaka, Japan). The qRT-PCR analysis was carried out using the SYBR Green Real-Time PCR Master Mix Kit (TOYOBO) and QuantStudio™ 6 Flex System (Applied Biosystems, Foster City, CA). The primer efficiency was checked by Bio-Rad CFX Manager software (Bio-Rad, Hercules, CA) within the range of 90 to 110%. The transcript level of each mRNA was normalized with the level of *BnaEF1α* and *BnaTubulin* mRNAs using the delta Ct method (Livak and Schmittgen, 2001), and their geometric means were shown as relative expression data (Vandesompele *et al.*, 2002). Gene-specific primers are listed in Table S4.

Vector construction and transformation in *B. napus*

To develop BnaA9.WRKY47 overexpressing plants, the full-length coding sequence of *BnaA9.WRKY47* amplified from 'Westar 10' was inserted into the PFGC5941 vector at the *AscI* and *PacI* restriction sites driven by the *CaMV35S* promoter. To create CRISPR/Cas9-mediated *BnaA9.WRKY47* targeted mutants, two target sequences sgRNA1 (AACTTGATAGAAAGTTACCGTGG) and sgRNA2 (ATCTTGACCACTACGTACGAAGG) were selected based on CRISPR-P (http://crispr.hzau.edu.cn/CRISPR/). The vectors (pKSE401 and pCBC-DT1T2) were used according to the method described by Xing *et al.* (2014). The plasmid constructs were then transferred into *Agrobacterium tumefaciens* GV3101 and were subsequently used to transform *B. napus* 'Westar 10' as described previously (De Block *et al.*, 1989). For overexpressing plants, three independent homozygous lines (35S#177, 184, 385) were selected from 11 lines based on phenotypic investigation under B deficiency, and qRT-PCR results verified the elevated expression of *BnaA9.WRKY47*. For CRISPR lines, the genomic region containing the two target sites was amplified and sequenced by *BnaA9.WRKY47*-specific primers (Table S4), a total of 19 independent mutant lines were obtained and three *BnaA9.WRKY47* homozygous mutants in the absence of *Cas9* transgene (CR#19, 24, 88) were selected for further study. The off-target detection was verified by sequencing the three most likely off-target sites in these lines (Table S3), and no sequence variations were detected in these regions.

Yeast one-hybrid assays

The yeast one-hybrid assays were performed using the Matchmaker One-Hybrid System following the manufacturer's instructions (Clontech, Mountain View, CA). The *WRKY* coding region was amplified from 'Westar 10' and cloned into the pGADT7-Rec2 prey vector by the In-Fusion HD Cloning kit (Takara Bio) to create a translational fusion between the GAL4 activation domain and the transcription factor. The bait sequence, four tandem copies of conserved W boxes or single copy of specific sequence from the target genes were synthesized (Tsingke Bio) and cloned into the pHIS2 reporter vector by *EcoRI* and *SacI*. The prey vector and reporter vector were cotransformed into the yeast strain Y187, and cotransformation of plasmids pGADT7-53 and pHIS2-53 were used as positive controls, while pGADT7-53 and pHIS2 empty vectors were negative controls. Cells were grown in SD/-Trp-Leu liquid media to an OD_{600} of 0.1 and then diluted with 10- and 100-fold sterile water. For each dilution, 7 μL was spotted on SD/-Trp-Leu-His media plates supplemented with 0 and 50 mM 3-AT (3-amino-1, 2,4-triazole, a competitive inhibitor of the yeast HIS3 protein, used to suppress background growth) to test the strength of the interaction. The plates were then incubated for 3–4 days at 30 °C.

Subcellular localization

For subcellular localization, the full-length coding sequence of *BnaA9.WRKY47* amplified from 'Westar 10' was cloned into the pM999-33 vector driven by the *CaMV35S* promoter (Tang *et al.*, 2016) using the In-Fusion HD Cloning kit (Takara Bio). The fused construct *35S:BnaA9.WRKY47:GFP* was cotransformed with *35S:Ghd7:CFP*, a nuclear marker (Tang *et al.*, 2016), into *Arabidopsis*

protoplasts. After transformation for 12 to 16 h, a confocal laser-scanning microscope (Leica SP8) was used for capturing the fluorescence signal with the setting of excitation/detection wavelengths: GFP (488 nm/505–540 nm) and CFP (448 nm/460-490 nm).

Electrophoretic mobility shift assay

The *BnaA9.WRKY47* full-length coding sequences were inserted into the inducible expression vector pET-15d (with 6 × His tag) using the In-Fusion HD Cloning kit (Takara Bio) and expressed in the *Escherichia coli* BL21 strain. Recombinant protein expression was induced with 0.2 mM isopropyl β-D-1-thiogalactopyranoside (IPTG) for 14 h at 16°C and further purified following the Sangon instructions (Ni-NTA Sefinose™ Resin, C600033). Two complementary oligonucleotide strands were labelled with 5′ Cy5 (Shanghai Sangon, China). The double-stranded oligonucleotides were generated by mixing with an equal amount of the complementary single-stranded oligonucleotides for 2 min at 95°C followed by cooling to 25°C. The labelled probes (1 μL of 10 μM/L mother probes) were incubated with the purified recombinant proteins (1–2 μg) in binding buffer (Beyotime, GS005) with or without unlabelled competitor DNA at 25 °C for 20 min. Finally, the DNA–protein complexes mixed with loading buffer (Beyotime, GS006) were electrophoresed on 6% nondenaturing polyacrylamide gels in the dark for 1 h at 4 °C. The fluorescence signal was captured by FLA-9000 (Fuji).

B concentration and MDA measurement

For B concentration measurement, the dried samples were ground into fine powders using a carnelian mortar, and B was lixiviated from 0.01 to 0.06 g powder in 1.0 M HCl (4–6 mL) by shaking (200 rpm) for 2 h. The B concentrations were measured by Inductively Coupled Plasma-Optical Emission Spectroscopy (ICP-OES, Varian, Inc.). Malondialdehyde (MDA) is a product of lipid peroxidation (Bejaoui *et al.*, 2016), and the degree of tissue damage by low B can be reflected by MDA concentration to a degree (Hua *et al.*, 2016b). For MDA determination, fresh samples (0.1–0.2 g) were ground with 5% TCA (1 mL) and the supernatant was added with an equal volume of 0.67% TBA. After incubation at 100°C for 30 min, the supernatant was measured by TECAN Infinite M200 under absorbances of 450 nm, 532 nm and 600 nm. The MDA content was calculated by the formula (nmol/L): 6.45*(A532-A600)-0.56*A450 (Bejaoui *et al.*, 2016).

Transient expression of proteins in tobacco cells and GUS activity measurements

A 3,176-bp DNA fragment upstream from the start codon of *BnaA3.NIP5;1* was amplified from 'Westar 10' and cloned into the PBI121 vector by *AscI* and *EcoRI* sites to generate *ProBnaA3.NIP5;1:GUS*. Transcription activation of *BnaA3.NIP5;1* by BnaA9.WRKY47 was detected by co-injecting *35S:BnaA9.WRKY47* and *proBnaA3.NIP5;1:GUS* into tobacco (*Nicotiana benthamiana*) leaves. For GUS staining, the leaves were infiltrated with staining solution (RealTimes, Beijing, China) for 12 h and decoloured in 75% ethanol. The GUS activity was quantitatively determined using the substrate 4-methylumbelliferyl-β-D-glucuronide (4-MUG), and the reaction product 4-methylymbelliferone (4-MU) was detected using TECAN Infinite M200. GUS activity was shown in units of nmol 4-methylumbelliferone produced per min per microgram of protein.

In situ hybridization

For in situ hybridization, seeds of *BnaA9.WRKY47* transgenic plants and wild-type were plated on MGRL solid medium (according to Fujiwara *et al.*, 1992) containing 100 μM B or 0.3 μM B, and were vertically grown in an incubator with a 16-h-light/ 8-h-dark cycle for 5 days. The 5-cm root tips were fixed with 50% FAA (5% formalin, 5% acetic acid, 45% ethanol and 45% water). To generate the *BnaA3.NIP5;1*-specific antisense probe, a 47-bp mRNA sequence fragment of *BnaA3.NIP5;1* was synthesized and labelled with DIG (digoxigenin): 5′-DIG-AACC-GAAUCAUAUAAAAAGCAAAGACGACACACAUAUGGAUGC-GUAC-3′ (Rochen Bio). The hybridization and immunological detection were performed as previously described (De Block and De Brouwer, 1993).

Statistical analysis

For statistical analyses, SPSS (Statistical Package for the Social Sciences) was used. Data are presented as means ± SD with at least three independent replicates. Significant differences were determined by *t*-test (* $P < 0.05$, ** $P < 0.01$, *** $P < 0.001$).

Sequences of primers and probes used in this study are listed in Table S4.

Acknowledgements

This work was funded by the National Natural Science Foundation of China (Grant No. 31772380, 31572185) and Fundamental Research Funds for the Central Universities of China (Grant No. 2662019PY058, 2662019PY013, 2662017QD039). We thank Prof. Lizhong Xiong (Huazhong Agricultural University, China) for providing the Y187 yeast strain and vectors for the Y1H assays, pM999-33 and Ghd7-CFP vectors for subcellular localization assays. We thank Prof. Ping Yin (Huazhong Agricultural University, China) for providing the strain and vectors for EMSA assays. We thank Prof. Qijun Chen (China Agricultural University, China) and Dr. Cheng Dai (Huazhong Agricultural University, China) for providing CRISPR system and the corresponding technical advising. We also thank Prof. Kede Liu (Huazhong Agricultural University, China) for providing PFGC5941 vector.

Conflict of interest

The authors declare no competing financial interests.

Author contributions

F.X. designed the research; Y.F., R.C., M.H., Y.H. and X.Y. performed the experiments and analysed the data; Y.F., F.X. and S.W. wrote the manuscript; L.S. reviewed the manuscript; all authors read and approved it.

References

Audic, S. and Claverie, J.M. (1997) The significance of digital gene expression profiles. *Genome Res.* **7**, 986–995.

Bejaoui, F., Salas, J.J., Nouairi, I., Smaoui, A., Abdelly, C., Martínez-Force, E. and Youssef, N.B. (2016) Changes in chloroplast lipid contents and chloroplast ultrastructure in *Sulla carnosa* and *Sulla coronaria* leaves under salt stress. *J. Plant Physiol.* **198**, 32–38.

De Block, M. and De Brouwer, D. (1993) RNA-RNA in situ hybridization using digoxigenin-labelled probes: the use of high-molecular-weight polyvinyl alcohol in the alkaline phosphatase indoxyl-nitroblue tetrazolium reaction. *Anal. Biochem.* **215**, 86–89.

De Block, M., De Brouwer, D. and Tenning, P. (1989) Transformation of *Brassica napus* and *Brassica oleracea* using Agrobacterium tumefaciens and the expression of the bar and neo genes in the transgenic plants. *Plant Physiol.* **91**, 694–701.

Cañon, P., Aquea, F., Rodríguez-Hoces de la Guardia, A. and Arce-Johnson, P. (2013) Functional characterization of *Citrus macrophylla BOR1*, as a boron transporter. *Physiol. Plant.* **149**, 329–339.

Chalhoub, B., Denoeud, F., Liu, S.Y., Parkin, I.A.P., Tang, H.B., Wang, X.Y., Chiquet, J. *et al*. (2014) Early allopolyploid evolution in the post-Neolithic *Brassica napus* oilseed genome. *Science*. **345**, 950–953.

Chatterjee, M., Tabi, Z., Galli, M., Malcomber, S., Buck, A., Muszynski, M. and Gallavotti, A. (2014) The boron efflux transporter rotten ear is required for maize inflorescence development and fertility. *Plant Cell*. **26**, 2962–2977.

Chen, Y.F., Li, L.Q., Xu, Q., Kong, Y.H., Wang, H. and Wu, W.H. (2009) The WRKY6 transcription factor modulates *PHOSPHATE1* expression in response to low Pi stress in *Arabidopsis*. *Plant Cell*. **21**, 3554–3566.

Cheng, F., Liu, S.Y., Wu, J., Fang, L., Sun, S.L., Liu, B., Li, P.X. *et al*. (2011) BRAD, the genetics and genomics database for *Brassica* plants. *BMC Plant Bio.* **11**, 136.

Chinnusamy, V., Schumaker, K. and Zhu, J.K. (2004) Molecular genetic perspectives on cross-talk and specificity in abiotic stress signalling in plants. *J. Exp. Bot.* **55**, 225–236.

Ciolkowski, I., Wanke, D., Birkenbihl, R.P. and Somssich, I.E. (2008) Studies on DNA-binding selectivity of WRKY transcription factors lend structural clues into WRKY-domain function. *Plant Mol. Biol.* **68**, 81–92.

Dai, X.Y., Wang, Y.Y. and Zhang, W.H. (2016) OsWRKY74, a WRKY transcription factor, modulates tolerance to phosphate starvation in rice. *J. Exp. Bot.* **67**, 947–960.

Devaiah, B.N., Karthikeyan, A.S. and Raghothama, K.G. (2007) WRKY75 transcription factor is a modulator of phosphate acquisition and root development in *Arabidopsis*. *Plant Physiol.* **143**, 1789–801.

Eulgem, T., Rushton, P.J., Robatzek, S. and Somssich, I.E. (2000) The WRKY superfamily of plant transcription factors. *Trends Plant Sci.* **5**, 199–206.

Fujiwara, T., Hirai, M.Y., Chino, M., Komeda, Y. and Naito, S. (1992) Effects of sulfur nutrition on expression of the soybean seed storage protein genes in transgenic petunia. *Plant Physiol.* **99**, 263–268.

Hanaoka, H., Uraguchi, S., Takano, J., Tanaka, M. and Fujiwara, T. (2014) OsNIP3;1, a rice boric acid channel, regulates boron distribution and is essential for growth under boron-deficient conditions. *Plant J.* **78**, 890–902.

He, Y.J., Mao, S.S., Gao, Y.L., Zhu, L.Y., Wu, D.M., Cui, Y.X., Li, J.N. *et al*. (2016) Genome-wide identification and expression analysis of WRKY transcription factors under multiple stresses in *Brassica napus*. *PLoS ONE*. **11**, e0157558.

Hoagland, D.R. and Arnon, D.I. (1950) The water-culture method for growing plants without soil. *Calif. Agr. Exp. Sta. Cir.* **347**, 1–39.

Hua, Y.P., Zhang, D.D., Zhou, T., He, M.L., Ding, G.D., Shi, L. and Xu, F.S. (2016a) Transcriptomics-assisted quantitative trait locus fine mapping for the rapid identification of a nodulin 26-like intrinsic protein gene regulating boron efficiency in allotetraploid rapeseed. *Plant Cell Environ.* **39**, 1601–1618.

Hua, Y.P., Zhou, T., Ding, G.D., Yang, Q.Y., Shi, L. and Xu, F.S. (2016b) Physiological, genomic and transcriptional diversity in responses to boron deficiency in rapeseed genotypes. *J. Exp. Bot.* **67**, 5759–5784.

Hua, Y.P., Feng, Y.N., Zhou, T. and Xu, F.S. (2017) Genome-scale mRNA transcriptomic insights into the responses of oilseed rape (*Brassica napus* L.) to varying boron availabilities. *Plant Soil*. **416**, 205–225.

Kasajima, I., Ide, Y., Yokota Hirai, M. and Fujiwara, T. (2010) WRKY6 is involved in the response to boron deficiency in *Arabidopsis thaliana*. *Physiol. Plant.* **139**, 80–92.

Leaungthitikanchana, S., Fujibe, T., Tanaka, M., Wang, S.L., Sotta, N., Takano, J. and Fujiwara, T. (2013) Differential expression of three *BOR1* genes corresponding to different genomes in response to boron conditions in hexaploid wheat (*Triticum aestivum* L.). *Plant Cell Physiol.* **54**, 1056–1063.

Livak, K.J. and Schmittgen, T.D. (2001) Analysis of relative gene expression data using real-time quantitative PCR and the 2(-Delta Delta C(T)) method. *Methods*. **25**, 402–408.

Marschner, P. (2012) *Marschner's mineral nutrition of higher plants*, 3rd ed. San Diego, CA: Academic Press.

Matthes, M.S., Robil, J.M., Tran, T., Kimble, A. and Mcsteen, P. (2018) Increased transpiration is correlated with reduced boron deficiency symptoms in the maize tassel-less1 mutant. *Physiol. Plant.* **163**, 344–355.

Miwa, K. and Fujiwara, T. (2010) Boron transport in plants: co-ordinated regulation of transporters. *Ann. Bot.* **105**, 1103–1108.

Nakagawa, Y., Hanaoka, H., Kobayashi, M., Miyoshi, K., Miwa, K. and Fujiwara, T. (2007) Cell-type specificity of the expression of OsBOR1, a rice efflux boron transporter gene, is regulated in response to boron availability for efficient boron uptake and xylem loading. *Plant Cell*. **19**, 2624–2635.

Noguchi, K., Yasumori, M., Imai, T., Naito, S., Matsunaga, T., Oda, H., Hayashi, H. *et al*. (1997) bor1-1, an *Arabidopsis thaliana* mutant that requires a high level of boron. *Plant Physiol.* **115**, 901–906.

Pérez-Castro, R., Kasai, K., Gainza-Cortés, F., Ruiz-Lara, S., Casaretto, J.A., Peña-Cortés, H., Tapia, J. *et al*. (2012) *VvBOR1*, the grapevine ortholog of *AtBOR1*, encodes an efflux boron transporter that is differentially expressed throughout reproductive development of *Vitis vinifera* L. *Plant Cell Physiol.* **53**, 485–494.

Phukan, U.J., Jeena, G.S. and Shukla, R.K. (2016) WRKY transcription factors: molecular regulation and stress responses in plants. *Front. Plant Sci.* **7**, 760.

Reiser, L., Subramaniam, S., Li, D.H. and Huala, E. (2017) Using the *Arabidopsis* Information Resource (TAIR) to find information about *Arabidopsis* genes. *Curr. Protoc. Bioinformatics*. **8**, 60.

Routray, P., Li, T., Yamasaki, A., Yoshinari, A., Takano, J., Choi, W.G., Sams, C.E. *et al*. (2018) Nodulin Intrinsic Protein 7;1 is a tapetal boric acid channel involved in pollen cell wall formation. *Plant Physiol.* **178**, 1269–1283.

Rushton, P.J., Somssich, I.E., Ringler, P. and Shen, Q.J. (2010) WRKY transcription factors. *Trends Plant Sci.* **15**, 247–258.

Shao, J.F., Yamaji, N., Liu, X.W., Yokosho, K., Shen, R.F. and Ma, J.F. (2018) Preferential distribution of boron to developing tissues is mediated by the intrinsic protein OsNIP3. *Plant Physiol.* **176**, 1739–1750.

Shorrocks, V.M. (1997) The occurrence and correction of boron deficiency. *Plant Soil*. **193**, 121–148.

Spitz, F. and Furlong, E.E. (2012) Transcription factors: from enhancer binding to developmental control. *Nature Rev. Genet.* **13**, 613–626.

Su, T., Xu, Q., Zhang, F.C., Chen, Y., Li, L.Q., Wu, W.H. and Chen, Y.F. (2015) WRKY42 modulates phosphate homeostasis through regulating phosphate translocation and acquisition in *Arabidopsis*. *Plant Physiol.* **167**, 1579–1591.

Takano, J., Noguchi, K., Yasumori, M., Kobayashi, M., Gajdos, Z., Miwa, K., Hayashi, H. *et al*. (2002) *Arabidopsis* boron transporter for xylem loading. *Nature*. **420**, 337–340.

Takano, J., Wada, M., Ludewig, U., Schaaf, G., von Wirén, N. and Fujiwara, T. (2006) The *Arabidopsis* major intrinsic protein NIP5;1 is essential for efficient boron uptake and plant development under boron limitation. *Plant Cell*. **18**, 1498–1509.

Tanaka, M., Wallace, I.S., Takano, J., Roberts, D.M. and Fujiwara, T. (2008) NIP6;1 is a boric acid channel for preferential transport of boron to growing shoot tissues in *Arabidopsis*. *Plant Cell*. **20**, 2860–2875.

Tanaka, M., Takano, J., Chiba, Y., Lombardo, F., Ogasawara, Y., Onouchi, H., Naito, S. *et al*. (2011) Boron-dependent degradation of *NIP5;1* mRNA for acclimation to excess boron conditions in *Arabidopsis*. *Plant Cell*. **23**, 3547–3559.

Tanaka, M., Sotta, N., Yamazumi, Y., Yamashita, Y., Miwa, K., Murota, K., Chiba, Y. *et al*. (2016) The minimum open reading frame, aug-stop, induces boron-dependent ribosome stalling and mRNA degradation. *Plant Cell*. **28**, 2830–2849.

Tang, N., Ma, S.Q., Zong, W., Yang, N., Lv, Y., Yan, C., Guo, Z.L. *et al*. (2016) MODD mediates deactivation and degradation of OsbZIP46 to negatively regulate ABA signaling and drought resistance in rice. *Plant Cell*. **28**, 2161–2177.

Ulker, B. and Somssich, I.E. (2004) WRKY transcription factors: from DNA binding towards biological function. *Curr. Opin. Plant Biol.* **7**, 491–498.

Vandesompele, J.De, Preter, K., Pattyn, F., Poppe, B., Van Roy, N., De Paepe, A. and Speleman, F. (2002) Accurate normalization of real-time quantitative RT-PCR data by geometric averaging of multiple internal control genes. *Genome Biol.* **3**, research0034.

Wang, H., Xu, Q., Kong, Y.H., Chen, Y., Duan, J.Y., Wu, W.H. and Chen, Y.F. (2014) Arabidopsis WRKY45 transcription factor activates PHOSPHATE TRANSPORTER1;1 expression in response to phosphate starvation. *Plant Physiol.* **164**, 2020–2029.

Wang, S.L., Yoshinari, A., Shimada, T., Hara-Nishimura, I., Mitani-Ueno, N., Ma, J.F., Naito, S. *et al*. (2017) Polar localization of the NIP5;1 boric acid channel is maintained by endocytosis and facilitates boron transport in *Arabidopsis* roots. *Plant Cell*. **29**, 824–842.

Xing, H.L., Dong, L., Wang, Z.P., Zhang, H.Y., Han, C.Y., Liu, B., Wang, X.C. *et al*. (2014) A CRISPR/Cas9 toolkit for multiplex genome editing in plants. *BMC Plant Biol.* **14**, 327.

Xu, F.S., Wang, Y.H., Ying, W.H. and Meng, J.L. (2002) Inheritance of boron nutrition efficiency in *Brassica napus*. *J. Plant Nut.* **25**, 901–912.

Yan, J.Y., Li, C.X., Sun, L., Ren, J.Y., Li, G.X., Ding, Z.J. and Zheng, S.J. (2016) A WRKY transcription factor regulates Fe translocation under Fe deficiency. *Plant Physiol.* **171**, 2017–2027.

Zhang, Q., Chen, H.F., He, M.L., Zhao, Z.Q., Cai, H.M., Ding, G.D., Shi, L. *et al*. (2017) The boron transporter BnaC4.BOR1;1c is critical for inflorescence development and fertility under boron limitation in *Brassica napus*. *Plant Cell Environ.* **40**, 1819–1833.

Supporting information

Additional supporting information may be found online in the Supporting Information section at the end of the article.

Figure S1 Validation of the random 10 *BnaWRKY* DEGs by qRT-PCR assays.
Figure S2 Co-expression network of *BnaWRKYs* in *B. napus*.
Figure S3 Microscopy of root tips. The plants were grown under 25 μM B and 0.25 μM B conditions for 15 days.
Figure S4 Transcript levels of *BnaBOR1s* in *BnaA9.WRKY47* transgenic lines.
Figure S5 BnaA9.WRKY47 binds to *BnaA3.NIP5;1* promoter by specific TGAC sequence in yeast.
Figure S6 BnaA9.WRKY47 binds to *BnaA3.NIP5;1* promoter by specific TGAC sequence in EMSA assays.
Table S1 The 51 *BnaWRKY* DEGs mRNA transcriptome data.
Table S2 The numbers of predicted WRKY-binding W boxes (T/CTGACC/T) in B stress-responsive genes.
Table S3 Examination of the sequences on putative off-target sites in *BnaA9.WRKY47* CRISPR/Cas9 mutants.
Table S4 Primer and probe sequences used in this study.

